MATHEMATICAL BIOSCIENCES
AND ENGINEERING
Volume **6**, Number **4**, October **2009**

doi:10.3934/mbe.2009.6.815

pp. **815–837**

MODELING TB AND HIV CO-INFECTIONS

Lih-Ing W. Roeger

Department of Mathematics and Statistics
Box 41042, Texas Tech University, Lubbock, TX 79409, USA

Zhilan Feng

Department of Mathematics
Purdue University, West Lafayette, IN 47907, USA

Carlos Castillo-Chavez

Department of Mathematics and Statistics
Arizona State University, Tempe, AZ 85287-1804, USA

(Communicated by Christopher Kribs-Zaleta)

Abstract. Tuberculosis (TB) is the leading cause of death among individuals infected with the human immunodeficiency virus (HIV). The study of the joint dynamics of HIV and TB present formidable mathematical challenges due to the fact that the models of transmission are quite distinct. Furthermore, although there is overlap in the populations at risk of HIV and TB infections, the magnitude of the proportion of individuals at risk for both diseases is not known. Here, we consider a highly simplified deterministic model that incorporates the joint dynamics of TB and HIV, a model that is quite hard to analyze. We compute independent reproductive numbers for TB ($\mathcal{R}_1$) and HIV ($\mathcal{R}_2$) and the overall reproductive number for the system, $\mathcal{R} = \max\{\mathcal{R}_1, \mathcal{R}_2\}$. The focus is naturally (given the highly simplified nature of the framework) on the qualitative analysis of this model. We find that if $\mathcal{R} < 1$ then the disease-free equilibrium is locally asymptotically stable. The TB-only equilibrium E_T is locally asymptotically stable if $\mathcal{R}_1 > 1$ and $\mathcal{R}_2 < 1$. However, the symmetric condition, $\mathcal{R}_1 < 1$ and $\mathcal{R}_2 > 1$, does not necessarily guarantee the stability of the HIV-only equilibrium E_H, and it is possible that TB can coexist with HIV when $\mathcal{R}_2 > 1$. In other words, in the case when $\mathcal{R}_1 < 1$ and $\mathcal{R}_2 > 1$ (or when $\mathcal{R}_1 > 1$ and $\mathcal{R}_2 > 1$), we are able to find a stable HIV/TB coexistence equilibrium. Moreover, we show that the prevalence level of TB increases with $\mathcal{R}_2 > 1$ under certain conditions. Through simulations, we find that i) the increased progression rate from latent to active TB in co-infected individuals may play a significant role in the rising prevalence of TB; and ii) the increased progression rates from HIV to AIDS have not only increased the prevalence level of HIV while decreasing TB prevalence, but also generated damped oscillations in the system.

1. **Introduction.** Tuberculosis is a bacterial disease caused by *M. tuberculosis* (a tubercle bacilli). TB is the leading cause of death among people infected with HIV [16]. Transmission of TB occurs by airborne spread of infectious droplets. The droplets are produced when a person with sputum smear-positive TB of the lung.

2000 *Mathematics Subject Classification.* Primary: 92D25, 92D30; Secondary: 34C60.
Key words and phrases. Tuberculosis, TB, HIV, disease reproduction number, co-infection.
The second author is partially supported by NSF grant DMS-0719697 .

TB is acquired through "interactions" with infectious individual, interactions that include primarily the sharing of a common "closed" environment. Once infected, a person stays infected for many years, possible latently-infected for life. Two billion people, about one-third of the world's total population were estimated to be infected with TB in 2006 [35].

HIV, the Human Immunodeficiency Virus, is the etiological agent responsible for the Acquired Immunodeficiency Syndrome (AIDS). HIV is not casually transmitted. There are multiple modes of HIV transmission including sexual intercourse, sharing needles with HIV-infected persons, or via HIV-contaminated blood transfusions. Infants may acquire HIV at delivery (birth) or through breast feeding if the mother is HIV positive. HIV severely weakens the immune system. Hence, it makes people highly vulnerable to invasions by a great number of infectious agents including mycobacterium, the etiological agent responsible for TB. There is a long, variable, latent period associated with HIV infection and the onset of HIV-related diseases including AIDS in adults. As HIV infection progresses, immunity declines and patients tend to become more susceptible to "common" or even rare infections. In many societies HIV and TB treatments are common today and the use of drugs have altered the joint dynamics of TB and HIV.

About one third of 39.5 million HIV-infected people worldwide are co-infected with TB [34] and up to 50 percent of individuals living with HIV are expected to develop TB [30, 33]. Many TB carriers who are infected with HIV are 30 to 50 times more likely to develop active TB than those without HIV [30]. The HIV epidemic has significantly impacted the dynamics of TB. In fact, one-third of the observed increases in active TB cases over the last five years can be attributed to the HIV epidemic [30]. For individuals infected with HIV, the presence of other infections, including TB tends to increase the rate of HIV replication. This acceleration may result in higher levels of infection and rapid HIV progression to the AIDS stage. The potential implications on the joint dynamics of HIV and TB will be explored in this paper.

Although the negative impact of the synergetic interactions between TB and HIV have caused worldwide concern, only a few statistical or mathematical models have been used to explore the consequences of their joint dynamics at the population level. There are plenty of single disease dynamic models. A significant number focus on TB [1, 3, 5, 6, 7, 9, 13, 14, 23] or on the transmission dynamics of HIV/AIDS [4, 17, 21, 29]. There are a few TB/HIV co-infection models (see for example [20, 22, 24, 25, 26, 27, 31]). Kirschner [20] developed a cellular model that described HIV-1 and TB co-infections inside a host. Naresh, et al. [22] developed a nonlinear mathematical model with the population divided into four sub classes: the susceptible, TB infective, HIV infective, and AIDS patients. Their model focused on the transmission dynamics of HIV and treatable TB in populations of varying sizes. Schulzer, et al. [27] studied HIV/TB joint dynamics using actuarial methods. West and Thompson [31] developed models for the joint dynamics of HIV and TB using numerical simulations to estimate parameters and predict the future transmission of TB in the United States. Porco, et al. [24] predict the potential impact of HIV on the probability and the expected severity of TB outbreaks using a discrete event simulation model.

Our approach differs from those found in the literature. Here, we focus on the joint dynamics of HIV and TB in a pseudo-competitive environment, at the population level. The model is not for a specific country or nation, and our approach does

not preclude the possibility of joint infections. The model assumes that invasions are bad news for each single host and that joint invasions are worse. This model is used to explore the impact of factors associated with co-infections on the prevalence of each of the two diseases. The possibility of HIV infections is incorporated within "typical" epidemiological frameworks that have been developed for the transmission dynamics of TB. The enhanced deterministic system is used to carry out a qualitative study of the joint transmission dynamics of TB and HIV.

This paper is organized as follows. In Section 2, we introduce a TB/HIV model that allows for the incorporation of both infections. We compute the *reproduction numbers* of each infectious disease and the overall reproduction number for the full system. Section 3 focuses on the study of boundary equilibria which include the disease-free state, the TB-free state, and the HIV-free state. The local stability of the disease-free and HIV-free equilibria are established. The existence of a possible co-existence equilibrium is also considered. Section 4 highlights the results of our analysis using selected numerical simulations. Section 5 discusses the relevance of the results presented in this manuscript and identifies possible future directions. The mathematical details are included in the appendix.

2. **The TB/HIV model.** A system of differential equations is introduced to model the joint dynamics of TB and HIV. The total population is divided into the following epidemiological subgroups: S, susceptible; L, latent with TB; I, infectious with TB; T, successfully treated with TB; J_1, HIV infectious; J_2, HIV infectious and TB latent; J_3, infectious with both TB and HIV; and A, "full-blown" AIDS. The compartmental diagram in Figure 1 illustrates the flow of individuals as they face the possibility of acquiring specific-disease infections or even co-infections.

The TB/HIV model is given by the following systems of eight ordinary differential equations:

$$
\begin{aligned}
TB &\begin{cases}
\frac{dS}{dt} = \Lambda - \beta c S \frac{I+J_3}{N} - \lambda\sigma S \frac{J^*}{R} - \mu S,\\
\frac{dL}{dt} = \beta c (S+T) \frac{I+J_3}{N} - \lambda\sigma L \frac{J^*}{R} - (\mu + k + r_1) L,\\
\frac{dI}{dt} = kL - (\mu + d + r_2) I,\\
\frac{dT}{dt} = r_1 L + r_2 I - \beta c T \frac{I+J_3}{N} - \lambda\sigma T \frac{J^*}{R} - \mu T,
\end{cases}\\
HIV &\begin{cases}
\frac{dJ_1}{dt} = \lambda\sigma (S+T) \frac{J^*}{R} - \beta c J_1 \frac{I+J_3}{N} - (\alpha_1 + \mu) J_1 + r^* J_2,\\
\frac{dJ_2}{dt} = \lambda\sigma L \frac{J^*}{R} + \beta c J_1 \frac{I+J_3}{N} - (\alpha_2 + \mu + k^* + r^*) J_2,\\
\frac{dJ_3}{dt} = k^* J_2 - (\alpha_3 + \mu + d^*) J_3,\\
\frac{dA}{dt} = \alpha_1 J_1 + \alpha_2 J_2 + \alpha_3 J_3 - (\mu + f) A,
\end{cases}
\end{aligned}
\tag{1}
$$

where

$$
\begin{aligned}
&N = S + L + I + T + J_1 + J_2 + J_3 + A,\\
&R = N - I - J_3 - A = S + L + T + J_1 + J_2,\\
&J^* = J_1 + J_2 + J_3.
\end{aligned}
\tag{2}
$$

The variable R denotes the "active" population that is the subgroup of individuals who do not have active TB or AIDS. The definitions of parameters are listed in Table 1.

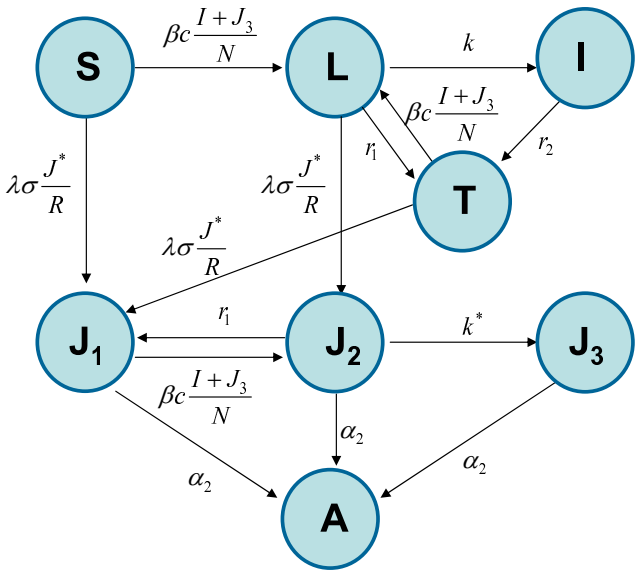

FIGURE 1. A transition diagram between epidemiological classes for the transmission dynamics of TB and HIV. All rates are per capita.

TABLE 1. Definitions of parameters and state variables used in the TB/HIV model (1).

Symbol	Definition
N	total population
R	total active population ($= N - I - J_3 - A = S + L + T + J_1 + J_2$)
J^*	Individuals with HIV who have not developed AIDS ($= J_1 + J_2 + J_3$)
Λ	constant recruitment rate
β	probability of TB infection per contact with a person with active TB
λ	probability of HIV infection per contact with a person with HIV
c	per-capita contact rate for TB
σ	per-capita contact rate for HIV
μ	per-capita natural death rate
k	per-capita TB progression rate for individuals not infected with HIV
k^*	per-capita TB progression rate for individuals infected also with HIV
d	per-capita TB-induced death rate
d^*	per-capita HIV-induced death rate
f	per-capita AIDS-induced death rate
r_1	per-capita latent TB treatment rate for individuals with no HIV
r_2	per-capita active TB treatment rate for individuals with no HIV
r^*	per-capita latent TB treatment rate for individuals with also HIV
α_i	per-capita AIDS progression rate for individuals in J_i ($i = 1, 2, 3$) class

The model is based on the following assumptions: the mixing between individuals is homogeneous; HIV individuals who are TB infectious (J_3) and exhibit severe HIV symptoms can not get an effective TB treatment; individuals get TB only through contacts with TB infectious individuals (I and J_3); and individuals may become HIV infected only through contacts with HIV infectious individuals (the J^* group). We assume also that the "probability" of infection per contact is the same for the T and S classes, namely β and λ. Further more, the I (TB infectious), J_3 (both TB and HIV infectious), and A (AIDS) individuals are considered too ill to remain sexually active and therefore they are unable to transmit HIV through sexual activity. $R \equiv N - I - J_3 - A$ denotes the "active" population and hence the "activity adjusted" HIV incidence is $\lambda\sigma J^*/R$ (see [8, 19, 36]). It appears that the function J^*/R might have a singularity at $R = 0$ as J^* includes J_3 while R does not. However, it is shown in the next section that the ratio J^*/R remains bounded for all time and, therefore, the system has no singularity.

We ignore important HIV transmission paths such as IV drug injections, vertically-transmitted HIV (children of birth), or HIV transmission via breast feeding. In other words, the probability of having a contact with HIV infectious individuals is modeled as J^*/R and the number of new HIV infections in a unit time is therefore $\lambda\sigma SJ^*/R$. Sexual-transmission is modeled as an indirect effect since the incorporation of modes of sexual interactions would make the model non-tractable analytically. Clearly, this last simplification is the most drastic. In addition, we do not include demography in the model which means that the time scale relevant to the model is tied in to time horizons where the demography has no serious impact.

The TB reproduction number (under treatment) is given by

$$\mathcal{R}_1 = \frac{\beta ck}{(\mu + k + r_1)(\mu + d + r_2)}, \tag{3}$$

and the HIV reproduction number is

$$\mathcal{R}_2 = \frac{\lambda\sigma}{\alpha_1 + \mu}. \tag{4}$$

Hence, the reproduction number for System (1) under TB treatment is

$$\mathcal{R} = \max\{\mathcal{R}_1, \mathcal{R}_2\}.$$

Both TB and HIV will die out if $\mathcal{R} < 1$ while either or both diseases may become endemic if $\mathcal{R} > 1$.

$\mathcal{R}_1$ is the product of the average number of susceptible infected by one TB infectious individual during his or her effective infectious period $\beta c/(\mu + d + r_2)$ times the fraction of the population that survives the TB latent period $k/(\mu + k + r_1)$. $\mathcal{R}_1$ gives the number of secondary TB infectious cases produced by a TB infectious individual during his or her effective infectious period when introduced in a population of mostly TB susceptibles (in the presence of treatment). $\mathcal{R}_2$ is the HIV reproduction number in the absence of TB, which gives the number of secondary HIV infectious produced by an HIV infectious (but not infected with TB) individual during his or her infectious period when introduced in a population of HIV susceptibles who have no TB.

Notice that the reproductive numbers defined above do not involve the parameters associated with individuals who are co-infected with both TB and HIV, e.g., k^* and α_3. In the following sections, we will explore the effect of these co-infection related parameters on the joint dynamics of the two diseases.

3. **Equilibria and local stability.** For System (1) the first octant in the state space is positively invariant, that is, solutions that start in this octant where all the variables are non-negative stay there. This can be verified as follows. Suppose, for example, at some time $\bar{t} > 0$ the variable L becomes zero, i.e., $L(\bar{t}) = 0$, while all other variables are positive. Then, from the L equation we have $dL(\bar{t})/dt > 0$. Thus, $L(t) \geq 0$ for all $t > 0$. Similarly, it can be shown that all variables remain nonnegative for all $t > 0$. Adding all the equations in Model (1) gives the following equation for N, the total population,

$$\frac{dN}{dt} = \Lambda - \mu N - (dI + d^* J_3 + fA).$$

Since $\frac{dN}{dt} < 0$, without loss of generality, we may consider only the solutions of System (1) that remain in the following positively invariant subset of R^8:

$$\Gamma = \Big\{(S, L, I, T, J_1, J_2, J_3, A) \;\Big|\; \begin{array}{l} S, L, I, T, J_1, J_2, J_3, A \geq 0, \\ S + L + I + T + J_1 + J_2 + J_3 + A \leq \frac{\Lambda}{\mu} \end{array}\Big\}.$$

For the continuity of the functions on the right-hand side of System (1), we only need to check the property of the ratio $J^*(t)/R(t)$, where $J^* = J_1 + J_2 + J_3$ and $R = N - I - J_3 - A = S + L + T + J_1 + J_2$. This is described in the following lemma.

Lemma 3.1. *The function* $\frac{J^*(t)}{R(t)}$ *is bounded for all* $t > 0$.

Proof. Since $J^*(t) \geq 0$ and $R(t) \geq 0$ for all $t > 0$, if $J^*(t)/R(t)$ is not bounded then a singularity occurs at some $\tilde{t} > 0$, at which

$$J^*(\tilde{t}) > 0 \quad \text{and} \quad R(\tilde{t}) = 0. \tag{5}$$

Notice that

$$\frac{J^*(t)}{R(t)} = \frac{J_1(t) + J_2(t) + J_3(t)}{S(t) + L(t) + T(t) + J_1(t) + J_2(t)}.$$

Thus, (5) implies that

$$S(\tilde{t}) = L(\tilde{t}) = T(\tilde{t}) = J_1(\tilde{t}) = J_2(\tilde{t}) = 0 \quad \text{and} \quad J_3(\tilde{t}) > 0. \tag{6}$$

From $R = N - I - J_3 - A$, we have

$$\begin{aligned} \frac{dR}{dt} &= \Lambda - \mu N - (dI + d^* J_3 + fA) - kL + (\mu + d + r_2)I - k^* J_2 \\ &\quad + (\alpha_3 + \mu + d^*)J_3 - (\alpha_1 J_1 + \alpha_2 J_2 + \alpha_3 J_3) + (\mu + f)A \\ &= \Lambda - \mu N - kL + (\mu + r_2)I - k^* J_2 + \mu J_3 - (\alpha_1 J_1 + \alpha_2 J_2) + \mu A. \end{aligned}$$

Using (6) and the fact that $N(t) \leq \Lambda/\mu$, we get

$$\begin{aligned} \frac{dR}{dt}\Big|_{t=\tilde{t}} &= \Lambda - \mu N(\tilde{t}) + \mu\big[I(\tilde{t}) + J_3(\tilde{t}) + A(\tilde{t})\big] + r_2 I(\tilde{t}) \\ &\geq \mu J_3(\tilde{t}) > 0. \end{aligned}$$

This, together with $R(\tilde{t}) = 0$ (see (5)), implies that $R(t) < 0$ for $t < \tilde{t}$ and near $\tilde{t}$. However, this contradicts the fact that $R(t) \geq 0$ for all $t > 0$. Therefore, $\frac{J^*(t)}{R(t)}$ is bounded for all $t > 0$. □

3.1. **Equilibria of a single disease or no disease.** System (1) has three possible nonnegative boundary equilibria in Γ: the disease-free equilibrium (DFE) denoted by E_0, the TB-only (HIV-free) equilibrium E_T, and the HIV-only (TB-free) equilibrium E_H. The components of E_0 are

$$S_0 = \frac{\Lambda}{\mu},\ L_0 = I_0 = T_0 = J_{01} = J_{02} = J_{03} = A_0 = 0.$$

At E_T, the components are

$$S_T = \frac{\Lambda}{\mu + \beta c I_T/N_T}, \quad L_T = \frac{I_T}{R_{1b}}, \quad I_T = \frac{N_T(\mathcal{R}_1 - 1)}{\mathcal{R}_1 + \mathcal{R}_{1a}}, \quad T_T = \frac{(r_1 L + r_2 I_T)S_T}{\Lambda},$$

$$J_{1T} = J_{2T} = J_{3T} = A_T = 0,$$

where

$$N_T = \frac{\Lambda}{\mu + d(\mathcal{R}_1 - 1)/(\mathcal{R}_1 + \mathcal{R}_{1a})},$$

with

$$\mathcal{R}_{1a} = \frac{\beta c}{\mu + k + r_1},\ \mathcal{R}_{1b} = \frac{k}{\mu + d + r_2}. \tag{7}$$

At E_H, the components are

$$S_H = \frac{\Lambda}{\mu\mathcal{R}_2 + \alpha_1(\mathcal{R}_2 - 1)}, \quad L_H = I_H = T_H = 0,$$

$$J_{1H} = (\mathcal{R}_2 - 1)S_H, \quad J_{2H} = J_{3H} = 0, \quad A_H = \frac{\alpha_1 J_{1H}}{\mu + f}.$$

It is easy to see that the HIV-free equilibrium E_T exists if and only if $\mathcal{R}_1 > 1$, and the TB-free equilibrium E_H exists if and only if $\mathcal{R}_2 > 1$. The stability of these boundary equilibria are described in the following results.

Theorem 3.2. *The disease-free equilibrium E_0 is locally asymptotically stable (LAS) if $\mathcal{R} < 1$, and it is unstable if $\mathcal{R} > 1$.*

A brief proof of Theorem 3.2 is given in the appendix. For the stability of E_T, the HIV-free equilibrium, we notice that α_1, α_2, and α_3 are the per-capita exit rates of individuals in the J_1 (HIV infectious), J_2 (HIV and TB latent), and J_3 (HIV and TB active) classes into the A class (AIDS). Therefore, it is reasonable to assume that $\alpha_1 \le \alpha_2 \le \alpha_3$, which implies that

$$\frac{\lambda\sigma}{\alpha_1 + \mu} \ge \frac{\lambda\sigma}{\alpha_2 + \mu} \ge \frac{\lambda\sigma}{\alpha_3 + \mu}.$$

Under these conditions, we have the following theorem for the local stability of E_T.

Theorem 3.3. *The HIV-free equilibrium E_T is LAS if $\mathcal{R}_1 > 1$ and $\mathcal{R}_2 < 1$.*

A proof of Theorem 3.3 is provided in the appendix. This result seems to be parallel with those found in the analysis of TB models without HIV ([6]). However, we need to point out that conditions stated in theorem 3.3, i.e., $\mathcal{R}_1 > 1$ and $\mathcal{R}_2 < 1$, are only sufficient but not necessary. In other words, our numerical simulations of the system (1) indicate that it is possible for E_T to be LAS even when $\mathcal{R}_2 > 1$ (see Section 4.3).

We remark that the symmetric conditions for the TB-free equilibrium E_H do not hold. That is, E_H may not be LAS under the conditions $\mathcal{R}_1 < 1$ and $\mathcal{R}_2 > 1$. Although we are not able to prove this analytically, our numerical studies show that

when $\mathcal{R}_1 < 1$ and $\mathcal{R}_2 > 1$ it is possible that the equilibrium E_H is unstable and TB can co-exist with HIV (see section 4.3).

3.2. **Interior equilibrium and their local stability.** When both reproduction numbers are greater than 1, i.e., $\mathcal{R}_1 > 1$ and $\mathcal{R}_2 > 1$, E_T and E_H both exist and E_0 is unstable. In this case, our numerical studies show that it is possible that all three boundary equilibria are unstable and solutions converge to an interior equilibrium point. Although explicit expressions for an interior equilibrium are very difficult to compute analytically, we have managed to obtain some relationships that can be used to determine the existence of an interior equilibrium.

Let $\hat{E} = (\hat{S}, \hat{L}, \hat{I}, \hat{J}_1, \hat{J}_2, \hat{J}_3, \hat{A})$ denote an interior equilibrium with all components positive, and let x and y denote the fractions in the incidence terms:

$$x = \frac{\hat{I} + \hat{J}_3}{\hat{N}} > 0 \quad \text{and} \quad y = \frac{\hat{J}^*}{\hat{R}} > 0. \tag{8}$$

The components of $\hat{E}$ can be determined by setting to zero of the right-hand side of the equations in (1):

$$\Lambda - \beta c\hat{S}x - \lambda\sigma\hat{S}y - \mu\hat{S} = 0, \tag{9}$$

$$\beta c(\hat{S} + \hat{T})x - \lambda\sigma\hat{L}y - (\mu + k + r_1)\hat{L} = 0, \tag{10}$$

$$k\hat{L} - (\mu + d + r_2)\hat{I} = 0, \tag{11}$$

$$r_1\hat{L} + r_2\hat{I} - \beta c\hat{T}x - \lambda\sigma\hat{T}y - \mu\hat{T} = 0, \tag{12}$$

$$\lambda\sigma(\hat{S} + \hat{T})y - \beta c\hat{J}_1 x - (\alpha_1 + \mu)\hat{J}_1 + r^*\hat{J}_2 = 0, \tag{13}$$

$$\lambda\sigma\hat{L}y + \beta c\hat{J}_1 x - (\alpha_2 + \mu + k^* + r^*)\hat{J}_2 = 0, \tag{14}$$

$$k^*\hat{J}_2 - (\alpha_3 + \mu + d^*)\hat{J}_3 = 0, \tag{15}$$

$$\alpha_1\hat{J}_1 + \alpha_2\hat{J}_2 + \alpha_3\hat{J}_3 - (\mu + f)\hat{A} = 0, \tag{16}$$

where $\hat{N} = \hat{S} + \hat{L} + \hat{I} + \hat{T} + \hat{J}_1 + \hat{J}_2 + \hat{J}_3 + \hat{A}$ and $\hat{R} = \hat{S} + \hat{L} + \hat{T} + \hat{J}_1 + \hat{J}_2$. From (9) we have

$$\hat{S} = \frac{\Lambda}{\mu + \beta cx + \lambda\sigma y}, \tag{17}$$

and from (10)-(12) we have

$$\begin{aligned} \hat{L} &= \frac{\hat{S}\beta c}{B_1}x = \frac{\beta c\Lambda}{B_1(\mu + \beta cx + \lambda\sigma y)}x, \\ \hat{I} &= \frac{k}{\mu + d + r_2}\hat{L}, \\ \hat{T} &= \frac{r_1 + \frac{r_2 k}{\mu + d + r_2}}{\beta cx + \lambda\sigma y + \mu}\hat{L}, \end{aligned} \tag{18}$$

where

$$\begin{aligned} B_1 &= \lambda\sigma y + \mu + k + r_1 - \frac{\beta cx(r_1 + \frac{r_2 k}{\mu + d + r_2})}{\beta cx + \lambda\sigma y + \mu} \\ &\geq \lambda\sigma y + \mu + k + r_1 - (r_1 + k) \\ &> 0. \end{aligned} \tag{19}$$

Thus, $\hat{S}, \hat{L}, \hat{I}$, and $\hat{T}$ can be determined by x and y. From the equations (13)-(15) we have

$$\begin{aligned}\hat{J}_1 &= \frac{\big(\hat{S}+\hat{T}+\frac{r^*\hat{L}}{\Delta_2}\big)\lambda\sigma y}{B_2},\\ \hat{J}_2 &= \frac{\hat{L}\lambda\sigma y + \hat{J}_1\beta c x}{\Delta_2},\\ \hat{J}_3 &= \frac{k^*(\hat{L}\lambda\sigma y + \hat{J}_1\beta c x)}{\Delta_2\Delta_3},\end{aligned} \tag{20}$$

where

$$\begin{aligned}\Delta_2 &= \alpha_2+\mu+k^*+r^*,\\ \Delta_3 &= \alpha_3+\mu+r^*+d,\\ B_2 &= \frac{\beta c x(\alpha_2+\mu+k^*)}{\Delta_2}+\alpha_1+\mu.\end{aligned} \tag{21}$$

Thus, $\hat{J}_i$ $(i=1,2,3)$ can be determined by x and y as well. Finally, from the equation (16),

$$\hat{A} = \frac{1}{\mu+f}\big(\alpha_1\hat{J}_1+\alpha_2\hat{J}_2+\alpha_3\hat{J}_3\big). \tag{22}$$

Thus, all components of $\hat{E}$ are functions of x and y. Clearly, $\hat{N}$ and $\hat{R}$ are also functions of x and y. Notice from (18) and (20) that $\hat{I}+\hat{J}_3$ is multiple of x, and $\hat{J}$ is multiple of y. In fact,

$$\hat{I}+\hat{J}_3 = \beta c x\Big[\frac{k\hat{S}}{(\mu+d+r_2)B_1}+\frac{k^*}{\Delta_2\Delta_3}\Big(\frac{\hat{S}\lambda\sigma y}{B_1}+\hat{J}_1\Big)\Big]$$

and

$$\begin{aligned}\hat{J} &= \hat{J}_1+\hat{J}_2+\hat{J}_3 = \hat{J}_1\Big(1+\frac{\beta c x}{\Delta_2}\big[1+\frac{k^*}{\Delta_3}\big]\Big)+\frac{\hat{L}\lambda\sigma y}{\Delta_2}\big[1+\frac{k^*}{\Delta_3}\big]\\ &= \lambda\sigma y\Big\{\frac{1}{B_2}\Big(\hat{S}+\hat{T}+\frac{r^*\hat{L}}{\Delta_2}\Big)\Big(1+\frac{\beta c x}{\Delta_2}\big[1+\frac{k^*}{\Delta_3}\big]\Big)+\frac{\hat{L}}{\Delta_2}\big[1+\frac{k^*}{\Delta_3}\big]\Big\}.\end{aligned}$$

Thus, from $x=(\hat{I}+\hat{J}_3)/\hat{N}$ and $y=\hat{J}^*/\hat{R}$, we know that x and y satisfy the following equations

$$\begin{aligned}x &= xF(x,y),\\ y &= yG(x,y),\end{aligned} \tag{23}$$

where

$$\begin{aligned}F(x,y) &= \frac{\beta c}{\hat{N}}\Big[\frac{k\hat{S}}{(\mu+d+r_2)B_1}+\frac{k^*}{\Delta_2\Delta_3}\Big(\frac{\hat{S}\lambda\sigma y}{B_1}+\hat{J}_1\Big)\Big],\\ G(x,y) &= \frac{\lambda\sigma}{\hat{R}}\Big\{\frac{1}{B_2}\Big(\hat{S}+\hat{T}+\frac{r^*\hat{L}}{\Delta_2}\Big)\Big(1+\frac{\beta c x}{\Delta_2}\big[1+\frac{k^*}{\Delta_3}\big]\Big)+\frac{\hat{L}}{\Delta_2}\big[1+\frac{k^*}{\Delta_3}\big]\Big\},\end{aligned} \tag{24}$$

in which, $\hat{S}$, $\hat{T}$, $\hat{L}$, $\hat{J}_1$, and B_i $(i=1,2)$ are functions of x and y as given in (17)-(21); and Δ_i $(i=2,3)$ are given in (19). Since $x\neq 0$ and $y\neq 0$ (as $\hat{I}>0$ and $\hat{J}^*>0$),

the equations in (23) can be simplified as

$$\begin{aligned} F(x,y) &= 1, \\ G(x,y) &= 1. \end{aligned} \tag{25}$$

From (17)-(22) we know that an interior equilibrium $\hat{E}$ corresponds to an intersection point (x,y) of the two curves $F=1$ and $G=1$ with $0<x<1$ and $y>0$ (it is possible that $y=\hat{J}^*/\hat{R}>1$ as J includes $\hat{J}_3$ while $\hat{R}$ does not). The two equations in (25) are very difficult to solve analytically due to the high nonlinearity of F and G. Nonetheless, we can numerically plot these two curves and examine how the intersection point(s) change with model parameters. For the choice of parameter values in our numerical studies, the literature offers useful information, see for example [12]. For numerical studies demonstrated in Figures 2–5, most of the parameters have fixed values while some will vary to demonstrate various cases in terms of extinction, persistence, or coexistence of the diseases. The fixed parameter values (the time unit is a year) are: $\mu=0.0143$ which corresponds to a life span of 70 years; $d=0.1$, $d^*=0.2$ and $f=0.5$ which imply that, after TB becomes active (not all TB-infected individuals reach the active stage), a person may die in ten years if no HIV or in 5 years or two years if the person also has HIV or AIDS; $k=0.5$ based on the assumption that the average latent period for TB is two years; $r_1=r^*=3$ and $r_2=1$, which correspond to the assumption that it will take four months and one year, respectively, for a latent and infectious person to become treated. Notice that the value r_1 maybe much smaller if a large proportion of latent TB individuals do not receive treatment. Similarly, the value of k may also be smaller if only a small fraction of latent TB individuals will develop active disease. In addition, $\alpha_1=0.1$ and $\alpha_2=2\alpha_1$, which imply that it takes on average 10 and 5 years for a person, who is infected with HIV only, or HIV and TB latent, to develop AIDS.

Notice that β and c always appear together and the product βc determines the TB reproduction number $\mathcal{R}_1$ given other parameters. We will consider different values of $\mathcal{R}_1$ by varying βc. Similarly, we will consider different values of HIV reproduction number $\mathcal{R}_2$ by varying the product $\lambda\sigma$. Notice also that the condition $k^*>k$ (i.e., the progression to active TB is faster in a person with HIV infection than without) reflects the influence that HIV may have on the dynamics of TB. Similarly, the condition $\alpha_i>\alpha_1$ $(i=2,3)$ (i.e., the progression to AIDS is faster in a person with TB infection than without) represents the influence of TB on the dynamics of HIV. We will examine how these conditions may affect the prevalence of the diseases. For demonstration purposes, the total population size used in all numerical studies is 10^4.

In Figure 2, the variable parameter values used are $\beta c=10$ (corresponding to $\mathcal{R}_1=1.3$) and $\lambda c=0.4$ (corresponding to $\mathcal{R}_2=3.5$); $k^*=5k$, which implies that the progression to TB in an individual who is also infected with HIV is five times higher; and $\alpha_3=5\alpha_1$, which implies that the rate of developing AIDS in a HIV person with TB is five times higher than without TB. In these figures, the surfaces of $F(x,y)$ and $G(x,y)$ are plotted and the curves $F(x,y)=1$ and $G(x,y)=1$ are shown as intersections of these surfaces with the plane of constant 1 (see Figure 2(A)(B)). In Figure 2(C), it is demonstrated that there is a unique point, $(\hat{x},\hat{y})=(0.27,0.096)$, at which $F(\hat{x},\hat{y})=G(\hat{x},\hat{y})=1$. Using (17)-(22) we can determine the components of the interior equilibrium $\hat{E}$.

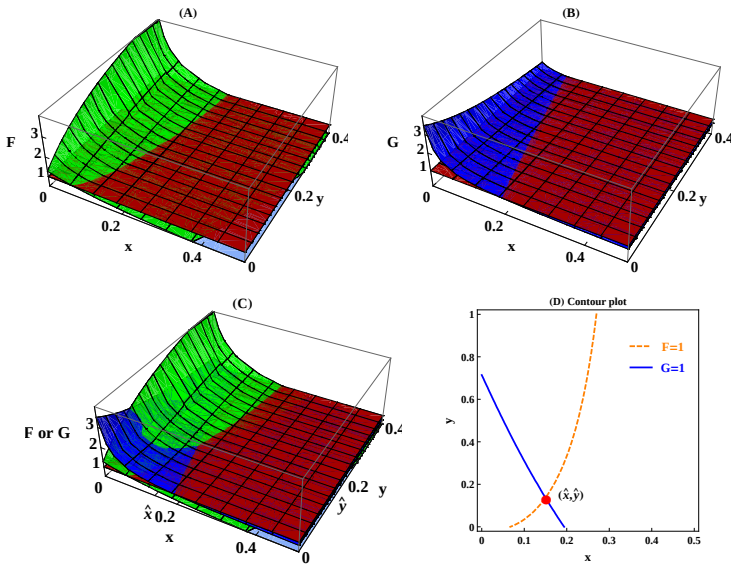

FIGURE 2. In (A) and (B) it is shown that there is a curve in the (x, y) plane along which $F(x, y) = 1$ and $G(x, y) = 1$, respectively. (C) illustrates that there is a unique point, $(\hat{x}, \hat{y}) = (0.14, 0.15)$, at which $F(\hat{x}, \hat{y}) = G(\hat{x}, \hat{y}) = 1$. This point determines an interior equilibrium $\hat{E}$. (D) shows the contour curves $F(x, y) = 1$ and $G(x, y) = 1$, and that there is a unique intersection point $(\hat{x}, \hat{y})$. The parameter values used are: $\beta c = 10$ (corresponding to $\mathcal{R}_1 = 1.3$), and $\lambda c = 0.4$ (corresponding to $\mathcal{R}_2 = 3.5$). Other parameter values used are: $\mu = 0.0143$, $d = 0.1$, $d^* = 0.2$, $k = 0.5$, $k^* = 5k$, $r_1 = 3$, $r_2 = 1$, $r^* = 3$, $\alpha_1 = 0.1$; $\alpha_2 = 0.2$, $\alpha_3 = 0.5$, and $f = 0.5$.

Figure 2 illustrates the existence of an interior equilibrium $\hat{E}$ when both reproduction numbers, $\mathcal{R}_1$ and $\mathcal{R}_2$, are greater than 1. The numerical simulations of the system suggest that the interior equilibrium is LAS in most cases. However, the simulations also suggest that stable periodic solutions are possible. Another interesting observation from the numerical studies of system (1) is that an interior equilibrium is possible even when $\mathcal{R}_1 < 1$, provided that the $\mathcal{R}_2 > 1$ (see Section 4.3).

4. **Numerical examples.** In this section we use model (1) to examine the impact that prevalence of HIV may have on TB dynamics and vice versa. We also present some numerical results on the stability of E_T (the HIV-free equilibrium) and E_H (the TB-free equilibrium).

One of the key parameters in the model to consider is k^*, which is the rate of TB progression in individuals who are co-infected with both HIV and latent TB. It has been reported that TB carriers who are infected with HIV are 30 to 50 times more likely to develop active TB than those without HIV [30]. This suggests that $k^* \geq k$, and in some cases, $k^* \gg k$. Our numerical studies indicate that only in certain cases, this factor may play an important role for explaining the effect of HIV epidemics on the increased prevalence level of TB.

4.1. **Impact of HIV on the prevalence level of TB infection.** In many epidemiological models, the magnitude of the reproduction number is associated with the level of infection. The same is true in model (1). That is, the reproduction numbers for TB and HIV, $\mathcal{R}_1$ and $\mathcal{R}_2$ (see (3) and (4)), are directly related to the infection levels of the respective diseases (in the absence of the other disease). Thus, we consider the impact of HIV on TB by first examining the effect of $\mathcal{R}_2$ on the prevalence of TB. Notice that both $\mathcal{R}_1$ and $\mathcal{R}_2 = \lambda\sigma/(\mu+\alpha_1)$ are independent of the parameters k^*, α_3, or f. Thus, we fix these parameters and $\mathcal{R}_1$ at various (given) values and look at changes in the levels of TB infections as $\mathcal{R}_2$ increases. Notice also that the x component of the two curves $F(x,y)$ and $G(x,y)$ (see $\hat{x} = (\hat{I} + \hat{J}_3)/\hat{N}$ in Figure 2) represents the fraction of individuals with active TB. We will consider $\hat{x}$ as a measure for the TB prevalence.

Figure 3 plots the intersection point $(\hat{x}, \hat{y})$ of the contour plots of $F(x,y) = 1$ (dashed curve) and $G(x,y) = 1$ (solid curve) for several values of $\mathcal{R}_2$ with $\mathcal{R}_1$ being fixed ($\mathcal{R}_1 = 1.5$ corresponding to $\beta c = 12$). Again, an interior equilibrium $\hat{E}$ can be determined by $\hat{x}$ and $\hat{y}$ if $0 < \hat{x} < 1$ and $\hat{y} > 0$. This figure illustrates how $\hat{x}$ changes with increasing $\mathcal{R}_2$. We have chosen $k^* = 5k$ (i.e., the progression rate to active TB in individuals with both latent TB and HIV is five times higher than that in individuals with latent TB only), $\alpha_3 = 5\alpha_1$ (i.e., the progression to AIDS in individuals with active TB is five times higher than that in individuals without TB), and $f = 1$. Other parameter values are the same as in Figure 2. The value of $\mathcal{R}_2$ in Figure 3(A)-(D) are 2.8, 3.6, 4.6, and 7, respectively. It shows that for smaller $\mathcal{R}_2$ the two curves do not have an intersection with positive x and y (see (A)); and thus, $\hat{E}$ does not exist. As $\mathcal{R}_2$ increases from 2.8 to 3.6, the $F(x,y) = 1$ curve does not change much while the right-end of the $G(x,y) = 1$ curve moves to the right of the $F = 1$ curve. This leads to an intersection point of the two curves (see (B)), which corresponds to an interior equilibrium $\hat{E}$. The right-end of the $G = 1$ curve moves up more as $\mathcal{R}_2$ is increased further to 4.6, and there is still a unique interior equilibrium with a larger x component (see (C)). Finally, when $\mathcal{R}_2$ is very large, the $G(x,y) = 1$ curve changes from decreasing to increasing. Although there is still a unique intersection point, the $y = \hat{J}^*/\hat{R}$ component may becomes greater than 1. This is still biologically feasible as J/R can exceed 1 (see (D)). The intersection points in (C)-(D) are $(\hat{x}, \hat{y}) = (\frac{\hat{I}+\hat{J}_3}{\hat{N}}, \frac{\hat{J}^*}{\hat{R}}) = (0.15, 0.07), (0.25, 0.4), (0.33, 1.25)$, respectively. We observe that $\hat{x}$ increases with $\mathcal{R}_2$ from 0.15 to 0.33. This implies that the prevalence of HIV may have significant impact on the infection level of TB.

We have also identified some scenarios in which the assumption $k^* > k$ does not automatically lead to an increase in TB prevalence. One of the reasons is that a person with both HIV and active TB (J_3) may progress at a faster rate ($\alpha_3 > \alpha_1$) to the AIDS stage (A) which is associated with an excess death rate ($f > 0$). In Figure 4 we examine the interplay between these factors.

In Figure 4(A)-(D), all parameters have the same values as in Figure 3(A)-(D) except that $k^* = 3k$ and $\alpha_3 = 10\alpha_1$. The intersection points in Figure 4(C)-(D) are $(\hat{x}, \hat{y}) = (\frac{\hat{I}+\hat{J}_3}{\hat{N}}, \frac{\hat{J}^*}{\hat{R}}) = (0.13, 0.07), (0.14, 0.28), (0.15, 0.65)$, respectively. It shows that although the y component of the intersection increases as $\mathcal{R}_2$ increases, the x component does not change much (from 0.13 to 0.15). This suggests that the condition $k^* > k$ alone may not be sufficient for HIV to have a significant impact on TB. Other factors may also play an important role, e.g., the development rate (α_3) to AIDS of individuals who are also infected with TB.

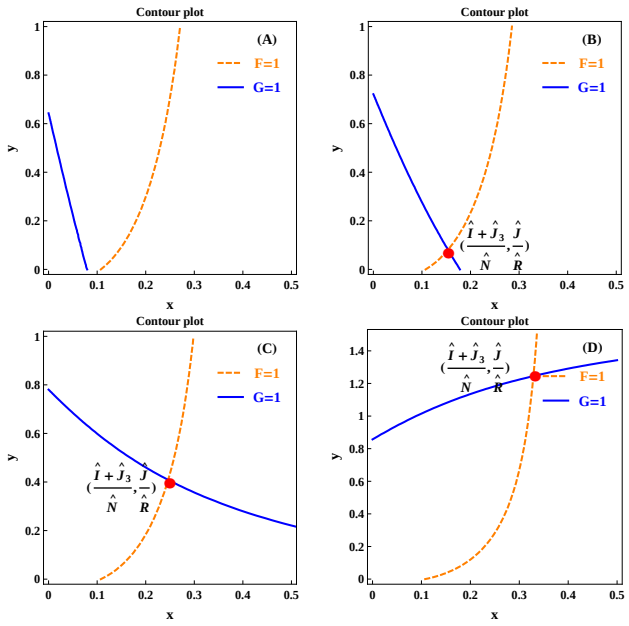

FIGURE 3. Contour plots showing the intersection points of the curves $F(x, y) = 1$ (dashed curve) and $G(x, y) = 1$ (solid curve) for various values of $\mathcal{R}_2$ with $\mathcal{R}_1$ fixed at 1.5 ($\beta c = 12$). The value of $\mathcal{R}_2$ in (A)-(D) are 2.8, 3.6, 4.6, and 7, respectively (corresponding to $\lambda\sigma = 0.32, 0.41, 0.52$, and 0.8). The axes are $x = (I + J_3)/N$ and $y = J^*/R$, representing the factors in the incidence functions for TB and HIV, respectively. The intersection $(\hat{x}, \hat{y}) = (\frac{\hat{I}+\hat{J}_3}{\hat{N}}, \frac{\hat{J}^*}{\hat{R}})$ determines components of the interior equilibrium $\hat{E}$ if $0 < \hat{x} < 1$ and $\hat{y} > 0$. It shows that for smaller $\mathcal{R}_2$ the two curves do not have an intersection with positive x and y (see (A)); and thus, $\hat{E}$ does not exist. As $\mathcal{R}_2$ increases from 2.8 to 3.6, the $F(x, y) = 1$ curve changes very little, while the right-end of the $G(x, y) = 1$ curve moves to the right of the $F = 1$ curve. This leads to an intersection point of the two curves (see (B)), which represents an interior equilibrium $\hat{E}$. The right-end of the $G = 1$ curve moves further up as $\mathcal{R}_2$ is increased to 4.6, and there is still a unique interior equilibrium with a larger x component (see (C)). Finally, when $\mathcal{R}_2$ is very large, the right-end of the $G(x, y) = 1$ curve continues to rise and it changes from decreasing to increasing. Although the y component of the unique intersection point is greater than one, it is still biologically feasible as $\hat{y} = \hat{J}/\hat{R}$ can exceed 1 (see (D)). All other parameter values are the same as in Figure 2.

Figure 5 examines changes in infection levels over time. It plots the time series of $[I(t)+J_3(t)]/N(t)$ (fraction of active TB) and $J^*(t)/R(t)$ (activity-adjusted fraction of HIV infectious) for fixed $\mathcal{R}_1$ and various $\mathcal{R}_2$. The top two figures are for the case when the reproduction number for TB is less then 1 ($\mathcal{R}_1 = 0.96 < 1$ or $\beta c = 7.5$), and the reproduction number for HIV is $\mathcal{R}_2 = 0.9 < 1$ (or $\lambda c = 0.105$) in (a) and

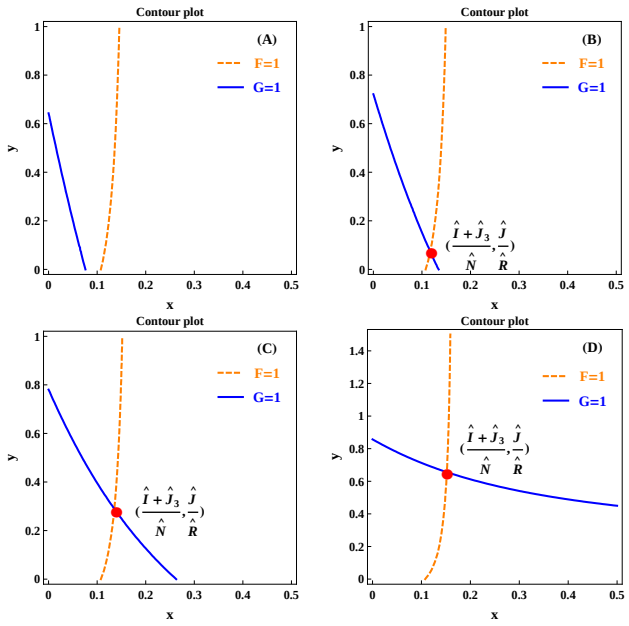

FIGURE 4. Contour plots similar to Figure 3 except that $k^* = 3k$ and $\alpha_3 = 10\alpha_1$. All other parameters have the same values as in Figure 3, i.e, $\mathcal{R}_1 = 1.5$ and $\mathcal{R}_2 = 2.8, 3.6, 4.6$, and 7 in (A)-(D), respectively. It shows that although $\hat{y} = \hat{J}/\hat{R}$ increases as $\mathcal{R}_2$ increases, $\hat{x} = (\hat{I}+\hat{J}_3)/\hat{N}$ does not change very much. This suggests that $k^* > k$ may not be sufficient for HIV to have a significant impact on TB. Other factors may also play an important role, e.g., the development rate (α_3) to AIDS in individuals who are also infected with TB.

$\mathcal{R}_2 = 1.3 > 1$ (or $\lambda c = 0.15$) in (a). It illustrates in Figure 5(a) that TB cannot persist if $\mathcal{R}_2 < 1$. However, if $\mathcal{R}_2 > 1$ then it is possible that TB can become prevalent even if $\mathcal{R}_1 < 1$ (see Figure 5(b)). The bottom two figures are for the case when the reproduction number of TB is greater than 1 ($\mathcal{R}_1 = 1.2$, or $\beta c = 9.1$), and $\mathcal{R}_2 = 2$ (or $\lambda c = 0.23$) in (c) and $\mathcal{R}_2 = 3$ (or $\lambda c = 0.34$) in (d). It demonstrates that an increase in $\mathcal{R}_2$ will lead to an increase in the level of TB prevalence as well. All other parameters are the same as in Figure 3 except that $k^* = 3k$.

Another way to look at the role of HIV on TB dynamics is to compare the outcomes between the cases where HIV is absent or present (instead of varying the value of $\mathcal{R}_2$). This result is presented in Figure 6. The reproduction numbers are identical in Figures 6(A)-(C): $\mathcal{R}_1 = 0.98 < 1$ ($\beta c = 7.7$) and $\mathcal{R}_2 = 1.2 > 1$ ($\lambda\sigma = 0.137$). Other parameter values are the same as in Figure 5 except that $k^* = k$. The variables plotted are $(I + J_2)/N$ and J^*/N. Figure 6(A) shows the case when HIV is absent by letting $J^*(0) = 0$. It shows that TB cannot persist. In Figure 6(B), the initial value of HIV is positive (i.e., $J^*(0) > 0$) but small. It shows that both TB and HIV will coexist. This seems to be similar to Figure 5(b) qualitatively. However, we observe that the prevalence level of TB remained low for a very long time (nearly 100 years) before rising and converging to the endemic

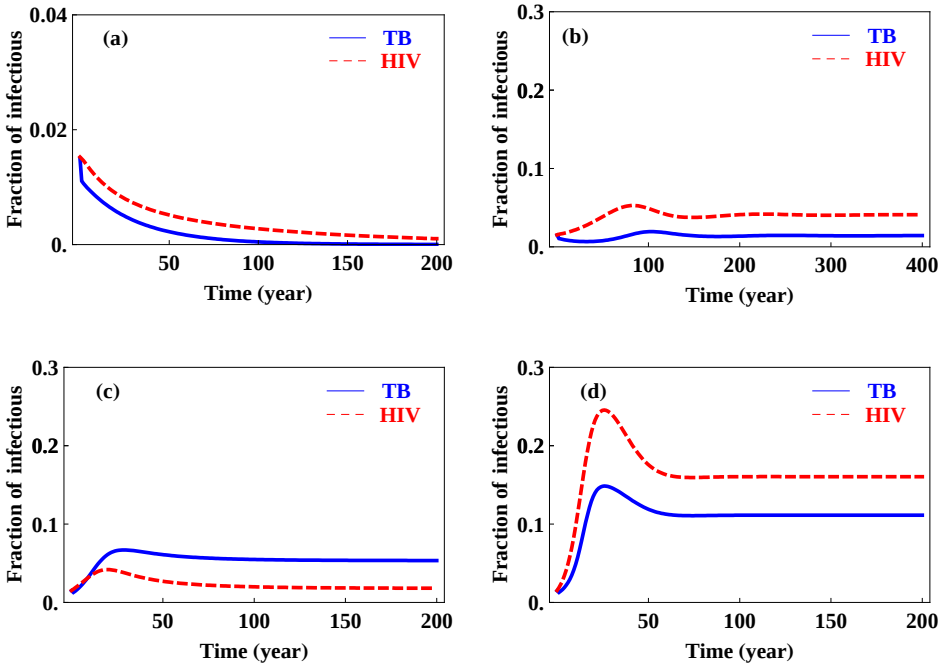

FIGURE 5. Time plots of prevalence of TB and HIV. The TB curves (solid) represents the fraction of active TB ($(I + J_3)/N$), and the HIV curve (dashed) represents the activity-adjusted fraction of HIV (J^*/R). In the top two figures, the reproduction number for TB is fixed and less then 1 ($\mathcal{R}_1 = 0.96$ or equivalently $\beta c = 7.5$), and the reproduction number for HIV is either less than 1 (see (a), $\mathcal{R}_2 = 0.9$ and equivalently $\lambda c = 0.105$) or greater than 1 (see (b), $\mathcal{R}_2 = 1.3$ and $\lambda c = 0.15$). Figure 5(a) illustrates that TB cannot persist if $\mathcal{R}_2 < 1$. Figure 5(b) shows that if $\mathcal{R}_2 > 1$ then it is possible that TB can become prevalent even though it cannot persist in the absence of HIV (as $\mathcal{R}_1 < 1$). The bottom two figures are for the case when the reproduction number of TB is greater than 1 ($\mathcal{R}_1 = 1.2$, or $\beta c = 9.1$), whereas the reproduction number for HIV is greater than 1 but either small (see Figure 5(c), $\mathcal{R}_2 = 2$ or $\lambda c = 0.23$) or large (see Figure 5(d), $\mathcal{R}_2 = 3$ or $\lambda c = 0.34$). It illustrates that an increase in $\mathcal{R}_2$ can lead to an increase in the prevalence level of TB. All other parameter values are the same as in Figure 3 except that $k^* = 3k$ and $\alpha_3 = 5\alpha_1$.

equilibrium. This phenomenon is not present when the initial value of HIV is larger, which is shown in Figure 6(C).

4.2. **Influence of TB on HIV dynamics.** Our numerical simulations also suggest that the presence of TB may have a significant impact on HIV dynamics. Some of the simulation results are demonstrated in Figure 7. This figure is similar to Figure 5 but shows time plots of $(I + J_3)/N$ (fraction of active TB) and J^*/R (activity-adjusted fraction of HIV infectious) for different values of α_i $(i = 1, 2, 3)$ (rates of

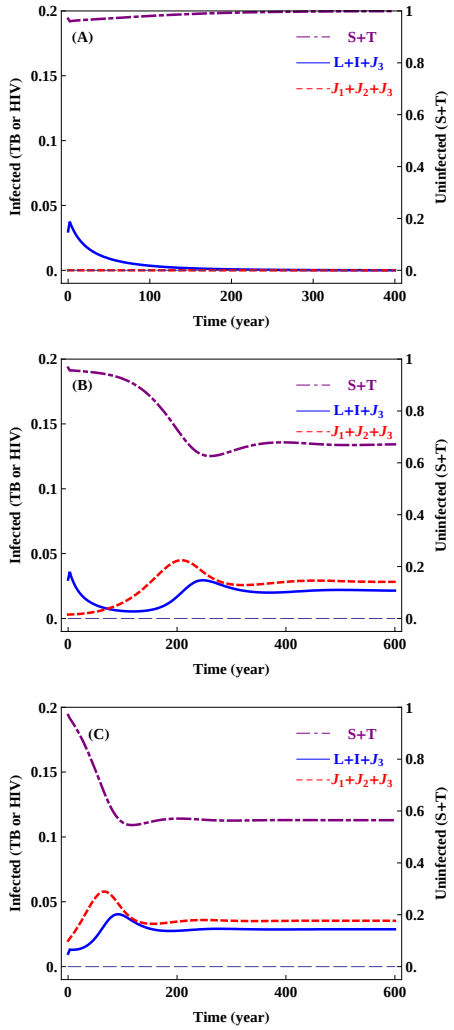

FIGURE 6. Demonstration of similar properties as shown in Figure 5 using a different approach. Instead of changing $\mathcal{R}_2$ as in Figure 5, different initial values of HIV are used in these figures. The reproduction numbers remain the same for Figure 6(A)-(C): $\mathcal{R}_1 = 0.98 < 1$ ($\beta c = 7.7$) and $\mathcal{R}_2 = 1.2 > 1$ ($\lambda\sigma = 0.137$). Other parameter values are the same as in Figure 5 except that $k^* = k$. The variables plotted are the fractions of active TB $(I+J_2)/N$ and HIV $((J_1 + J_2 + J_3)/N)$. In Figure 6(A), HIV is absent by letting $J^*(0) = 0$. It shows that TB cannot persist. In Figure 6(B), the initial value of HIV is positive (i.e., $J^*(0) > 0$) but small. It shows that both TB and HIV will coexist, with a lower level of TB for a quite long period of time before stabilizing at the equilibrium. This phenomenon is not present when the initial value of HIV is larger, which is shown in Figure 6(C).

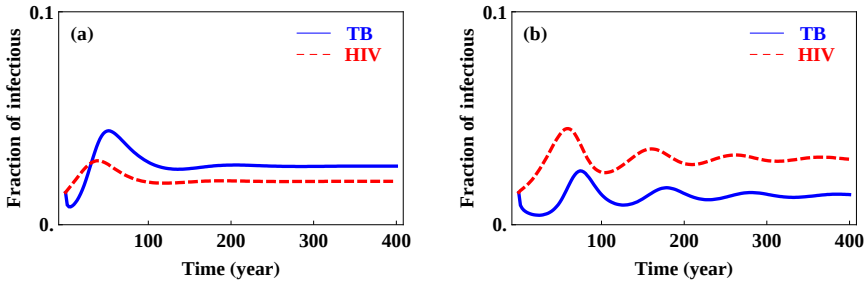

FIGURE 7. Time plots of $(I+J_3)/N$ and J^*/R for different values of α_i (rates of AIDS development, $i = 1, 2, 3$). Figure 7(a) is for the case of $\alpha_2 = \alpha_3 = \alpha_1$ (i.e., progression from HIV to AIDS is the same for a person with or without TB infection), while Figure 7(b) is for the case of $\alpha_2 = 2\alpha_1$ and $\alpha_3 = 5\alpha_1$ (i.e., for TB latent and TB active individuals, the progression from HIV to AIDS is respectively two and five times faster than a person without TB infection). In both plots, $\mathcal{R}_1 = 0.8$ ($\beta c = 6.3$) and $\mathcal{R}_2 = 1.5$ ($\lambda\sigma = 0.097$). All other parameter values are the same as in Figure 5 except that $r^* = 0.5r$ (i.e., it takes twice as long to treat a latently infected person with HIV than without) and $\alpha_1 = 0.05$. It shows that the increased progression rates due to TB have not only increased the prevalence level of HIV while decreasing TB prevalence, but also generated damped oscillations in the system.

AIDS development). Figure 7(a) is for the case of $\alpha_2 = \alpha_3 = \alpha_1$ (i.e., progression from HIV to AIDS is the same for a person with or without TB infection), while Figure 7(b) is for the case of $\alpha_2 = 2\alpha_1$ and $\alpha_3 = 5\alpha_1$ (i.e., for TB latent and TB active individuals, the progression from HIV to AIDS is respectively two and five times faster than a person without TB infection). The reproductive numbers are the same for both plots: $\mathcal{R}_1 = 0.8$ ($\beta c = 6.3$) and $\mathcal{R}_2 = 1.5$ ($\lambda\sigma = 0.097$). All other parameter values are the same as in Figure 5 except that $r^* = 0.5r$ (i.e., it takes twice as long to treat a latently infected person with HIV than without) and $\alpha_1 = 0.05$. It shows that the increased progression rates due to TB have not only increased the prevalence level of HIV while decreasing TB prevalence, but also generated damped oscillations in the system.

We remark that the incidence function $\lambda c J^*/R$ in the system (1) may have contributed to the oscillatory behavior of the system, as has been reported in previous studies (see [15, 18, 36]). However, we have also performed similar simulations of system (1) with the incidence function $\lambda\sigma J^*/R$ being replaced by the standard incidence $\lambda\sigma J^*/N$. We found that the damped oscillations are still present (see Figure 8). For demonstration purposes, we have changed some of parameter values: $r_1 = 0.3$, $r^* = 0.2r_1$, $k = 0.05$, $\alpha_1 = 0.05$. All other parameters have the same values as in Figure 5. The reproductive numbers are: $\mathcal{R}_1 = 0.85$ ($\beta c = 6.85$) and $\mathcal{R}_2 = 1.5$ ($\lambda\sigma = 0.097$). This suggests that the oscillatory behavior of the system is not necessarily generated by the use of the non-standard incidence. There are also parameter regions in which the system has stable periodic solutions. These cases are not presented here as the parameter values that generate periodic solutions are not biologically feasible.

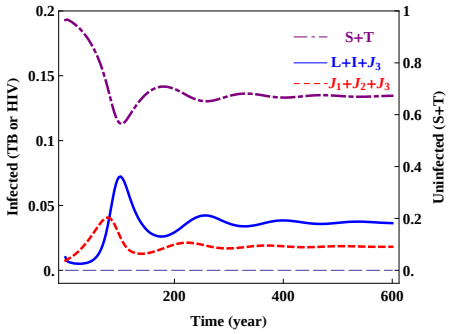

FIGURE 8. Similar to Figure 7 but for the system in which the incidence function in (1) for HIV, $\lambda\sigma J^*/R$, is replaced by the standard incidence $\lambda\sigma J^*/N$. It shows that the damped oscillations are still present.

4.3. **More on stability conditions for boundary equilibria E_T and E_H.** Recall that in section 3.1 we pointed out that the conditions, $\mathcal{R}_1 > 1$ and $\mathcal{R}_2 < 1$, in Theorem 3.3 for the stability of E_T are sufficient but not necessary, and that the symmetric conditions, $\mathcal{R}_1 < 1$ and $\mathcal{R}_2 > 1$, may not guarantee the stability of E_H. Our numerical simulations provide examples for i) E_T can still be stable under the conditions $\mathcal{R}_1 > 1$ and $\mathcal{R}_2 > 1$ (see Figure 9); and ii) E_H may not be stable when $\mathcal{R}_1 > 1$ and $\mathcal{R}_2 < 1$ (see Figures 5 and 6).

Figure 9(A) demonstrates an example that solutions may converge to E_T when $\mathcal{R}_1 > 1$ and $\mathcal{R}_2 > 1$, if $\mathcal{R}_2$ is not too large (for this plot $\mathcal{R}_1 = 1.15$ or $\beta c = 9$, and $\mathcal{R}_2 = 1.1$ or $\lambda\sigma = 0.126$). Figure 9(B) illustrates that as $\mathcal{R}_2$ increases, E_T becomes unstable and an interior equilibrium exists and is stable. The reproduction numbers in Figure 9(B) are $\mathcal{R}_1 = 1.1$ ($\beta c = 8.6$) and $\mathcal{R}_2 = 1.5$ ($\lambda\sigma = 0.171$). In Figure 9(C), $\mathcal{R}_2$ is increased to 1.75, and it shows that the HIV is also increased. All other parameters are the same as in Figure 2.

Figure 5(B), Figures 6(B), and 6(C) all demonstrate the scenario in which TB can coexist with HIV even when $\mathcal{R}_1 < 1$, provided that HIV is present and $\mathcal{R}_2 > 1$. We also observe that the prevalence of TB may be very low when HIV is low (see Figure 6(B)). However, an increase in HIV prevalence will also increase the level of infection for TB (see Figure 6(C)).

5. **Discussion.** TB is the leading cause of HIV-related morbidity and mortality. In fact, HIV infection often results in increases in the prevalence of active TB. We explored a model that incorporates the impact of TB and HIV co-infections. We constructed the bare-bone model in the most simple settings possible. We ignored the important HIV transmission paths such as vertically-transmitted HIV and HIV transmission via breast feeding. This model provides rather general insights into the potential effects of HIV infection on TB and vice versa. Detailed models that take into accounts various forms of TB treatment (latent and active TB), the danger of increasing the prevalence of antibiotic resistant TB and their relation to HIV treatment, observed changes in behavior of sexually-active core groups now that HIV "treatment" is available, and explicitly modeled sexual-transmission must be incorporated into models of HIV/TB co-infection if further progress is to be made.

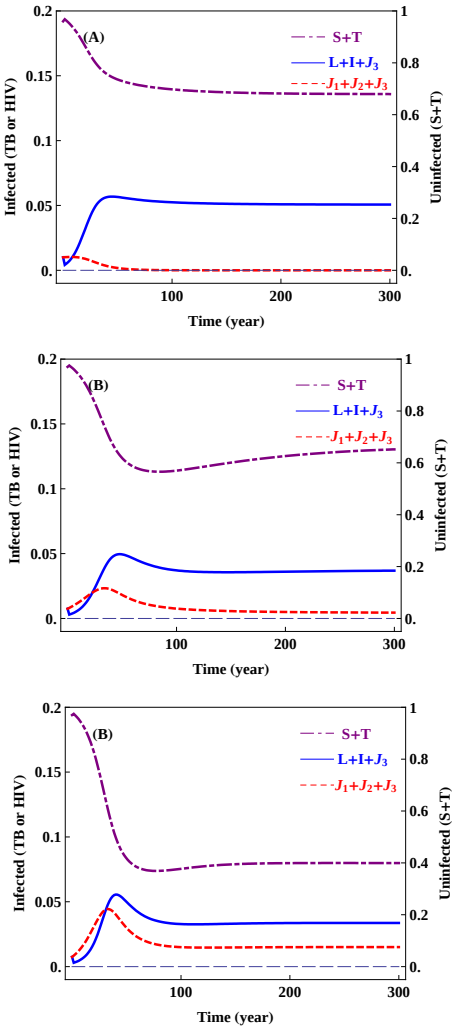

FIGURE 9. Figure 9(A) demonstrates that solutions may converge to the HIV-free equilibrium E_T when $\mathcal{R}_1 > 1$ and $\mathcal{R}_2 > 1$ (for this figure $\mathcal{R}_1 = 1.15$ and $\mathcal{R}_2 = 1.1$). Figure 9(B) illustrates that when $\mathcal{R}_2$ is larger than $\mathcal{R}_1$ (for this figure $\mathcal{R}_1 = 1.1$ and $\mathcal{R}_2 = 1.5$), E_T becomes unstable and solutions converge to an interior equilibrium. In Figure 9(C), $\mathcal{R}_2$ is increased to 1.75 and it shows that the HIV level is also increased.

The full model (1) is an 8-dimensional system for which only limited analytical results are obtained. We are able to compute independent reproduction numbers for TB ($\mathcal{R}_1$) and HIV ($\mathcal{R}_2$) and the total reproduction number for the system, $\mathcal{R} = \max\{\mathcal{R}_1, \mathcal{R}_2\}$. We find that if $\mathcal{R} < 1$ the disease-free equilibrium is locally asymptotically stable. The HIV-free equilibrium with only TB present is stable if $\mathcal{R}_1 > 1$ and $\mathcal{R}_2 < 1$. However, the symmetric result does not hold. That is, the TB-free equilibrium may not be stable $\mathcal{R}_1 < 1$ and $\mathcal{R}_2 > 1$. In fact, our simulation

results show that co-existence of both diseases is possible when $\mathcal{R}_1 < 1$ and $\mathcal{R}_2 > 1$ (see Figure 5(b)). Although we do not have an explicit expression for the possible interior equilibrium $\hat{E}$, we managed to derive a pair of equations which can be used to determine the existence of $\hat{E}$ (see equations (25)). Numerical studies suggest that the system has a unique interior equilibrium when $\mathcal{R} > 1$ (see Figure 2).

The simulation results provided many interesting insights into the effect of the dynamical interactions between TB and HIV. For example, the results illustrated in Figures 3 and 5 show that, when the progression from latent to active TB is faster in people with HIV than in people without (i.e., $k^* > k$), the presence of HIV can lead to the coexistence of TB and HIV even if the TB reproduction number ($\mathcal{R}_1$) is below 1 (i.e., TB infection would not be able to establish itself in the absence of HIV). However, the condition $k^* > k$ does not always lead to a significant increase in TB in the presence of HIV. The results illustrated in Figure 4 suggest that if $\alpha_3 >> \alpha_1$ (i.e., the development of HIV to AIDS is much faster in individuals co-infected with TB than without) then the effect of k^* will be diminished or not dramatic. However, simulation results presented in Figures 7 and 8 suggest that when $\alpha_i > \alpha_1$, $i = 2, 3$), the presence of TB may have a significant influence on HIV dynamics. Moreover, increasing α_2 and α_3 may lead to oscillatory behaviors of the system.

Numerical results suggest that to reduce or control the impact of TB, investing more in reducing the prevalence of HIV can be an effective option. Such reductions would not be easy due to the lack of effective vaccine and medication. However, significant reductions may be obtained through programs that accelerate the treatment of active TB cases. Since there are about 8 million new cases of active TB per year, a program may be feasible. It has worked in countries that allocate substantial resources to public health. Naturally, accelerating the treatment rate of individuals with active TB is more critical in areas where HIV prevalence is high. Unfortunately, the areas with the highest prevalence of co-infections have limited resources and cannot implement accelerated TB treatment programs.

It is worth stressing that our models and observations are rather crude for multiple reasons. The results are not only based on local mathematical analysis but they are from a model that does not incorporate multiple and common forms of HIV transmission, the possibility of increases in antibiotic resistant TB, and the impact of human behavior, particularly the role of core groups (prostitution, drug uses, etc.) A research program that tackles some of these possibilities is still viable since the dynamics of co-infection is not well studied and therefore they are still poorly understood from a theoretical or mathematical perspective.

Acknowledgments. We would like to thank the referees very much for their valuable comments and suggestions.

REFERENCES

[1] J. P. Aparicio, A. F. Capurro and C. Castillo-Chavez, *Markers of disease evolution: the case of tuberculosis*, J. Theor. Biol., **215** (2002), 227–237.

[2] B. R. Bloom, "Tuberculosis: Pathogenesis, Protection, and Control," ASM Press, Washington D. C., 1994.

[3] S. Blower, P. Small and P. Hopewell, *Control strategies for tuberculosis epidemics: New models for old problems*, Science, **273** (1996), 497–500.

[4] C. Castillo-Chavez, *Review of recent models of HIV/AIDS transmission*, in "Applied Mathematical Ecology" (ed. S. Levin), Biomathematics Texts, Springer-Verlag, **18** (1989), 253–262.

[5] C. Castillo-Chavez and Z. Feng, *Mathematical models for the disease dynamics of tuberculosis*, in "Advances in Mathematical Population Dynamics-Molecules, Cells and Man" (eds. Mary Ann Horn, G. Simonett and G. Webb), Vanderbilt University Press, 1998, 117–128.
[6] C. Castillo-Chavez and Z. Feng, *To treat or not to treat: The case of tuberculosis*, J. Math. Biol., **35** (1997), 629–656.
[7] C. Castillo-Chavez and Z. Feng, *Global stability of an age-structure model for TB and its applications to optimal vaccination*, Math. Biosci., **151** (1998), 135–154.
[8] C. Castillo-Chavez, H. W. Hethcote, V. Andreasen, S. A. Levin and W. Liu, *Cross-immunity in the dynamics of homogeneous and heterogeneous populations*, in "Mathematical Ecology" (ed. Trieste), World Sci. Publishing, Teaneck, NJ, 1988, 303-316.
[9] C. Castillo-Chavez and B. Song, *Dynamical models of tuberculosis and their applications*, Math. Biosci. and Engineering, **1** (2004), 361–404.
[10] O. Diekmann, K. Dietz and J. A. P. Heesterbeek, *The basic reproduction ration for sexually transmitted diseases: I. Theoretical considerations*, Math. Biosci., **107** (1991), 325–339.
[11] O. Diekmann, J. A. P. Heesterbeek and J. A. J. Metz, *On the definition and the computation of the basic reproduction ration $\mathcal{R}_0$ in models for infectious diseases in heterogeneous populations*, J. Math. Biol., **28** (1990), 365–382.
[12] C. Dye, S. Scheele, P. Dolin, V. Pathania and M. C. Raviglione, *Consensus statement. Global burden of tuberculosis: Estimated incidence, prevalence, and mortality by country*, in "WHO Global Surveillance and Monitoring Project," *JAMA*, **282** (1999), 677–686.
[13] Z. Feng and C. Castillo-Chavez, *A model for Tuberculosis with exogenous reinfection*, Theor. Pop. Biol., **57** (2000), 235–247.
[14] Z. Feng, W. Huang and C. Castillo-Chavez, *On the role of variable latent periods in mathematical models for tuberculosis*, J. Dynam. Differential Equations, **13** (2001), 425–452.
[15] Z. Feng and H. R. Thieme, *Recurrent outbreaks of childhood diseases revisited: The impact of isolation*, Math. Biosci., **128** (1995), 93–129.
[16] P. Godfrey-Faussett, D. Maher, Y. Mukadi, P. Nunn, J. Perriens and M. Raviglione, *How human immunodeficiency virus voluntary testing can contribute to tuberculosis control*, Bulletin of the World Health Organization, **80** (2002), 939–945.
[17] H. W. Hethcote, "Modeling HIV transmission and AIDS in the United States," Lecture Notes in Biomathematics, Springer-Verlag, New York, 1992.
[18] H. W. Hethcote, Z. Ma and S. Liao, *Effects of quarantine in six endemic models for infectious diseases*, Math. Biosci., **180** (2002), 141–160.
[19] K. Koelle, S. Cobey, B. Grenfell and M. Pascual, *Epochal evolution shapes the phylodynamics of interpandemic influenza A (H3N2) in humans*, Science, **314** (2006), 1898–1903.
[20] D. Kirschner, *Dynamics of co-infection with M. tuberculosis and HIV-1*, Theor. Pop. Biol., **55** (1999), 94–109.
[21] R. M. May and R. M. Anderson, *The transmission dynamics of human immunodeficiency virus (HIV)*, in "Applied Mathematical Ecology" (ed. S. Levin), Biomathematics Texts, **18**, Springer-Verlag, New York, 1989.
[22] R. Naresh and A. Tripathi, *Modelling and analysis of HIV-TB Co-infection in a variable size population*, Mathematical Modelling and Analysis, **10** (2005), 275–286.
[23] T. Porco and S. Blower, *Quantifying the intrinsic transmission dynamics of tuberculosis*, Theor. Pop. Biol., **54** (1998), 117–132.
[24] T. Porco, P. Small and S. Blower, *Amplification dynamics: Predicting the effect of HIV on tuberculosis outbreaks*, Journal of Acquired Immune Deficiency Syndromes, **28** (2001), 437–444.
[25] S. M. Raimundo, A. B. Engel, H. M. Yang and R. C. Bassanezi, *An approach to estimating the transmission coefficients for AIDS and for tuberculosis using mathematical models*, Systems Analysis Modelling Simulation, **43** (2003), 423–442.
[26] R. B. Schinazi, *Can HIV invade a population which is already sick?* Bull. Braz. Math. Soc. (N.S.), **34** (2003), 479–488.
[27] M. Schulzer, M. P. Radhamani, S. Grybowski, E. Mak and J. M. Fitzgerald, *A mathematical model for the prediction of the impact of HIV infection on tuberculosis*, Int. J. Epidemiol., **23** (1994), 400–407.
[28] K. Styblo, *Selected papers: Epidemiology of tuberculosis*, Royal Netherlands Tuberculosis Association, 24 (1991), 55–62.
[29] H. R. Thieme and C. Castillo-Chavez, *How may infection-age infectivity affect the dynamics of HIV/AIDS?*, SIAM J. Appl. Math., **53** (1993), 1447–1479.

[30] "Tuberculosis and AIDS: UNAIDS Point of View," UNAIDS, Geneva, October, 1997.
[31] R. West and J. Thompson, *Modeling the impact of HIV on the spread of tuberculosis in the United States*, Math. Biosci., **143** (1997), 35–60.
[32] "Global Tuberculosis Control, WHO Report 2001," World Health Organization, Geneva, Switzerland, 2001, WHO/CDS/TB/2001.287.
[33] "Strategic Frame Work to Decrease the Burden of TB/HIV," World Health Organization, Geneva, Switzerland, March, 2002.
[34] WHO, http://www.who.int/hiv/mediacentre/02-Global_Summary_2006_EpiUpdate_eng.pdf, Geneva, Switzerland, 2006.
[35] WHO, Tubercusosis Facts, http://www.who.int/tb/publications/2007/factsheet_2007.pdf, 2007.
[36] L.-I. Wu and Z. Feng, *Homoclinic bifurcation in an SIQR model for childhood diseases*, J. Diff. Equations, **168** (2000), 150–167.

6. **Appendix.** Some details of the proofs of results associated with system (1) are provided.

Proof of Theorem 3.2. To establish the local stability, we can use the classical method of the Jacobian matrix or use the approach of the next generation operator [10, 11].

At the disease-free equilibrium E_0, the total population N is equal to the total susceptible S population. The Jacobian matrix at E_0 has eigenvalues $-\mu$, $-\mu$, $-(\mu+f)$, $\lambda\sigma-\alpha_1-\mu$, $-(\alpha_2+\mu+k^*+r^*)$, $-(\alpha_3+\mu+d^*)$, and two other numbers, z_1 and z_2, which are the roots of the quadratic equation in w

$$z^2+\big(2\mu+k+d+r_1+r_2\big)z+\big[(\mu+k+r_1)(\mu+d+r_2)-\beta ck\big]=0.$$

The eigenvalues z_i will have a negative real part whenever $\lambda\sigma-\alpha_1-\mu<0$ and $(\mu+k+r_1)(\mu+d+r_2)-\beta ck>0$, that is, if $\mathcal{R}_1<1$ and $\mathcal{R}_2<1$ where $\mathcal{R}_1$ and $\mathcal{R}_2$ are given in (3) and (4). Since

$$\mathcal{R}=\max\{\mathcal{R}_1,\mathcal{R}_2\},$$

we see that if $\mathcal{R}<1$ then the disease-free equilibrium E_0 is LAS. □

Proof of Theorem 3.3. We let $W=S+T$ and observe that the system (1) is equivalent to the following set of equations:

$$\begin{aligned}
N' &= \Lambda-\mu N-dI-d^*J_3-fA,\\
L' &= \beta c(N-L-I-J^*-A)\frac{I+J_3}{N}-\lambda\sigma L\frac{J^*}{R}-(\mu+k+r_1)L,\\
I' &= kL-(\mu+d+r_2)I,\\
J_1' &= \lambda\sigma(N-L-I-J^*-A)\frac{J^*}{R}-\beta cJ_1\frac{I+J_3}{N}-(\alpha_1+\mu)J_1+r^*J_2,\\
J_2' &= \lambda\sigma L\frac{J^*}{R}+\beta cJ_1\frac{I+J_3}{N}-(\alpha_2+\mu+k^*+r^*)J_2,\\
J_3' &= k^*J_2-(\alpha_3+\mu+d^*)J_3,\\
A' &= \alpha_1J_1+\alpha_2J_2+\alpha_3J_3-(\mu+f)A,
\end{aligned}\tag{26}$$

where $R=N-I-J_3-A$ and $J^*=J_1+J_2+J_3$. The Jacobian matrix at E_T has the form:

$$M_J=\begin{bmatrix} M_1 & * & * \\ 0 & M_2 & 0 \\ 0 & * & -(\mu+f)\end{bmatrix},$$

where M_1 and M_2 are both 3×3 matrices and $*$ denotes some nonzero element that does not affect the analysis. The matrix M_1 is

$$M_1 = \begin{bmatrix} -\mu & 0 & -d \\ a(\mathcal{R}_1 - 1) & -(a\mathcal{R}_1 + \mu + k + r_1) & \dfrac{\beta c}{\mathcal{R}_1} - a\mathcal{R}_1 \\ 0 & k & -(\mu + d + r_2) \end{bmatrix}, \text{ where } a = \frac{\beta c I}{\mathcal{R}_1 N}.$$

The characteristic polynomial of M_1 is $x^3 + Ax^2 + Bx + C = 0$ where

$$\begin{aligned} A &= a\mathcal{R}_1 + 3\mu + k + r_1 + r_2 + d, \\ B &= a\mathcal{R}_1(2\mu + k + r_2 + d) + \mu(2\mu + k + r_1 + r_2 + d), \\ C &= \mu a\mathcal{R}_1(\mu + k + r_2 + d) + kad(\mathcal{R}_1 - 1). \end{aligned}$$

We observe that $A > 0$, $C > 0$ and $AB > C$. Then based on the Routh-Hurwitz criteria, we see that the eigenvalues of M_1 all have negative real parts as long as $\mathcal{R}_1 > 1$.

The matrix M_2 is

$$M_2 = \begin{bmatrix} -(K + \omega_1) & X + r^* & X \\ K & -(X + \omega_2 + k^* + r^*) & \lambda\sigma - X \\ 0 & k^* & -(\omega_3 + \lambda\sigma + d^*) \end{bmatrix},$$

where $X = \lambda\sigma\frac{W}{R}$, $K = \lambda\sigma\frac{L}{R} + \beta c\frac{I}{N}$, and $\omega_i = \alpha_i + \mu - \lambda\sigma\,(i = 1, 2, 3)$. Note that $\mathcal{R}_2 < 1$ implies that $\omega_i > 0$ for $i = 1, 2, 3$, then the characteristic polynomial of M_2 is $x^3 + A_1x^2 + B_1x + C_1 = 0$, where

$$\begin{aligned} A_1 = {} & \lambda\sigma + \omega_1 + \omega_2 + \omega_3 + r^* + d^* + k^* + X + K, \\ B_1 = {} & (d^* + \lambda\sigma + \omega_2 + \omega_3 + k^*)K + (\lambda\sigma + k^* + \omega_1 + \omega_3 + d^*)X \\ & + \lambda\sigma(\omega_1 + \omega_2 + r) \\ & + (\omega_1\omega_2 + \omega_1\omega_3 + \omega_2\omega_3) + \omega_2 d^* + \omega_1 k^* + \omega_1 r^* + \omega_3 r^* \\ & + r^* d^* + \omega_1 d^* + \omega_3 k^* + k^* d^*, \\ C_1 = {} & (k^* d^* + \omega_2 d^* + \omega_2\omega_3 + \omega_2\lambda\sigma + k^*\omega_3)K + (\omega_1\omega_3 + \omega_1\lambda\sigma + \omega_1 d^* + \omega_1 k^*)X \\ & + \omega_1 r^* d^* + r^*\omega_1\omega_3 + k^* d^*\omega_1 + k^*\omega_1\omega_3 + d^*\omega_1\omega_2 + \omega_1\omega_2\omega_3 \\ & + r^*\lambda\sigma\omega_1 + \lambda\sigma\omega_1\omega_2. \end{aligned}$$

Therefore $A_1 > 0$ and $C_1 > 0$. We can also show that $A_1B_1 > C_1$ (using **Maple**) and therefore, we conclude that the Routh-Hurwitz stability criterion is satisfied by M_2. In other words, all eigenvalues of M_2 have negative real parts. We have therefore shown that all eigenvalues of M_J have negative real parts as long as $\mathcal{R}_1 > 1$ and $\mathcal{R}_2 < 1$. We conclude that the HIV-free equilibrium E_T is locally asymptotically stable if $\mathcal{R}_1 > 1$ and $\mathcal{R}_2 < 1$. □

Received October 25, 2007; Accepted June 14 2009.

E-mail address: lih-ing.roeger@ttu.edu
E-mail address: zfeng@math.purdue.edu
E-mail address: ccchavez@asu.edu